ABCG1 regulates pulmonary surfactant metabolism in mice and men[S]

Thomas Q. de Aguiar Vallim,[*,†,§,] Elinor Lee,[*,††] David J. Merriott,[1,†] Christopher N. Goulbourne,[§§] Joan Cheng,[†] Angela Cheng,[†] Ayelet Gonen,[***] Ryan M. Allen,[2,†††] Elisa N. D. Palladino,[†††,§§§] David A. Ford,[†††,§§§] Tisha Wang,[*,††] Ángel Baldán,[†††] and Elizabeth J. Tarling[3,*,§,**]**

Department of Medicine,* Department of Biological Chemistry, David Geffen School of Medicine,† Molecular Biology Institute,§ Johnson Comprehensive Cancer Center,** and Division of Pulmonary and Critical Care Medicine,†† University of California Los Angeles, Los Angeles, CA 90095; Columbia Nano Initiative Electron Microscopy Facility,§§ Columbia University, New York, NY 10027; Department of Medicine,*** University of California San Diego, La Jolla, CA 92093; and Edward A. Doisy Department of Biochemistry and Molecular Biology††† and Center for Cardiovascular Research, School of Medicine,§§§ Saint Louis University, St. Louis, MO 63104

ORCID ID: 0000-0002-0599-0432 (E.J.T.)

Abstract Idiopathic pulmonary alveolar proteinosis (PAP) is a rare lung disease characterized by accumulation of surfactant. Surfactant synthesis and secretion are restricted to epithelial type 2 (T2) pneumocytes (also called T2 cells). Clearance of surfactant is dependent upon T2 cells and macrophages. ABCG1 is highly expressed in both T2 cells and macrophages. ABCG1-deficient mice accumulate surfactant, lamellar body-loaded T2 cells, lipid-loaded macrophages, B-1 lymphocytes, and immunoglobulins, clearly demonstrating that ABCG1 has a critical role in pulmonary homeostasis. We identify a variant in the *ABCG1* promoter in patients with PAP that results in impaired activation of *ABCG1* by the liver X receptor α, suggesting that ABCG1 basal expression and/or induction in response to sterol/lipid loading is essential for normal lung function. We generated mice lacking ABCG1 specifically in either T2 cells or macrophages to determine the relative contribution of these cell types on surfactant lipid homeostasis. These results establish a critical role for T2 cell ABCG1 in controlling surfactant and overall lipid homeostasis in the lung and in the pathogenesis of human lung disease.—de Aguiar Vallim, T. Q., E. Lee, D. J. Merriott, C. N. Goulbourne, J. Cheng, A. Cheng, A. Gonen, R. M. Allen, E. N. D. Palladino, D. A. Ford, T. Wang, Á. Baldán, and E. J. Tarling. **ABCG1 regulates pulmonary surfactant metabolism in mice and men. *J. Lipid Res.* 2017.** 58: **941–954.**

Supplementary key words cholesterol • phospholipid • lung • pulmonary alveolar proteinosis • ATP binding cassette transporter G1

Surfactant is a complex mixture of lipids and proteins that forms a monolayer lining the alveolar sacs in the lungs to maintain surface tension and prevent the collapse of alveoli (1). Surfactant is composed of ~85% phospholipids [predominantly dipalmitoyl phosphatidylcholine (PC)], ~10% neutral lipids (mostly cholesterol), and ~5% proteins. The latter include surfactant proteins (SPs), SP-A, SP-B, SP-C, and SP-D. These proteins play critical roles in the formation, function, and metabolism of surfactant (2–5). SP-A and SP-D also play critical roles in the immune response to foreign antigens (3–6).

Surfactant lipids are synthesized and secreted by epithelial type 2 (T2) pneumocytes (also called T2 cells). Initially, lipids and SPs, SP-B and SP-C, are packed into lamellar bodies, specialized secretory organelles within T2 cells, prior to fusion with the plasma membrane and secretion into the hypophase of the alveoli (7). Other proteins recovered in surfactant, including SP-A and SP-D, are secreted

This work was supported, in part, by National Heart, Lung, and Blood Institute Grants HL116181 (to E.J.T.), HL122677 (to T.Q.d.A.V.), and HL107794 (to A.B.); National Institute of General Medical Sciences Grant GM115553 (to D.A.F.); American Heart Association Grant-in-Aid 13BGIA17080038 (to E.J.T.); and Scientist Development Grant 14SDG18440015 (to T.Q.d.A.V.). The content is solely the responsibility of the authors and does not necessarily represent the official views of the National Institutes of Health.

The authors declare no conflicts of interest.

Manuscript received 23 January 2017 and in revised form 3 March 2017.

Published, JLR Papers in Press, March 6, 2017
DOI https://doi.org/10.1194/jlr.M075101

Copyright © 2017 by the American Society for Biochemistry and Molecular Biology, Inc.

This article is available online at http://www.jlr.org

Abbreviations: Ad-ABCG1, ABCG1 adenovirus; BAL, broncho-alveolar lavage; BM, bone marrow; HF/HC, high fat/high cholesterol; LXR, liver X receptor; PAP, pulmonary alveolar proteinosis; PC, phosphatidylcholine; PE, phosphatidylethanolamine; PG, phosphatidylglycerol; SP, surfactant protein; T2, type 2.

[1]Present address of D. J. Merriott: Department of Radiation-Oncology, Stanford School of Medicine, Stanford, CA 94305.

[2]Present address of R. M. Allen: Department of Medicine, Vanderbilt University Medical Center, Nashville, TN 37232.

[3]To whom correspondence should be addressed.
e-mail: etarling@mednet.ucla.edu

[S] The online version of this article (available at http://www.jlr.org) contains a supplement.

through a different lamellar body-independent pathway (8). It is estimated that most of the surfactant phospholipids are synthesized in situ by T2 cells, whereas cholesterol is derived from serum lipoproteins with less than 1% being derived from de novo synthesis (9).

The mechanisms involved in subsequent clearing of the extracellular surfactant are not fully understood. It is known that both T2 cells and alveolar macrophages participate in the uptake of lipids from the alveolar hypophase in a process mediated by SP-A and SP-D (2, 8, 10). T2 cells recycle most of these lipids, repackaging them into lamellar bodies prior to resecretion. In contrast, surfactant phospholipids taken up by macrophages are thought to be catabolized. Intratracheal administration of radiolabeled dipalmitoyl PC suggests that T2 cells and macrophages contribute equally to surfactant uptake and/or degradation in vivo (11).

ABCG1 is a member of the ABC family of transmembrane transporters [reviewed in (12–15)]. ABCG1 has been shown to facilitate cholesterol efflux from cells to a variety of exogenous lipid acceptors that include LDL, phospholipid vesicles, phospholipid/apolipoprotein complexes, and mature HDL, but not lipid-poor apoA1 (16–23). We have demonstrated that ABCG1 localizes to intracellular organelles of the endosomal pathway, where it functions to regulate intracellular sterol homeostasis (24, 25). This is consistent with work from Sturek et al. (26), who reported that ABCG1 is important for pancreatic β-cell cholesterol homeostasis and insulin secretion.

Abcg1$^{-/-}$ mice have normal plasma lipid levels, but exhibit an age-related progressive pulmonary disease that has many of the properties associated with human respiratory distress syndromes, including lipidosis and chronic inflammation (27–30). Although the lungs of young mice (<6 weeks) appear visually normal, they are already accumulating small amounts of lipid. By the age of 6–8 months, the lungs of chow-fed *Abcg1*$^{-/-}$ mice are white as a result of lipid accumulation within macrophages and T2 cells and in the extracellular spaces (17, 27, 28, 30). The lungs of aged *Abcg1*$^{-/-}$ mice contain large numbers of lipid-loaded macrophages and 5-fold more T2 cells (28). Compared with T2 cells in wild-type mice, T2 cells in *Abcg1*$^{-/-}$ mice contain 5-fold more lamellar bodies that are both larger and more dense, consistent with intracellular accumulation of surfactant lipids that likely contributes to the overall pulmonary lipidosis (28). In addition, the lungs of *Abcg1*$^{-/-}$ mice show evidence of inflammation, as judged by increased lymphocytic infiltration, increased expression of cytokines, and the presence of chitinase-3-like crystals (27, 28, 30). All these changes are greatly accelerated when *Abcg1*$^{-/-}$ mice were fed a Western diet containing 21% fat and 0.2% cholesterol (17, 28). In contrast to the abnormalities of macrophages and T2 cells in the lungs of *Abcg1*$^{-/-}$ mice, endothelial cells and type 1 epithelial cells that line the alveoli appear normal, as determined by standard lipid staining techniques and electron microscopy (17, 28).

Taken together, these studies identified pivotal roles for ABCG1 in controlling pulmonary homeostasis in vivo (17, 27, 28, 30, 31). Interestingly, functional loss of two other ABC transporters (ABCA3 and ABCA1) also results in pulmonary lipid abnormalities (32, 33). Loss of ABCA3 results in early postnatal death in both humans and mice due to the inability of *Abca3*$^{-/-}$ T2 cells to package surfactant into lamellar bodies and subsequently secrete these lipid organelles into the hypophase (33–35). In contrast, loss of ABCA1 (Tangier disease) results not only in >95% loss in plasma HDL in mice and humans, but also in a mild pulmonary lipidosis in mice (32). To our knowledge, pulmonary lipidosis has not been described in Tangier patients (36, 37).

In order to determine whether ABCG1 has a cell-autonomous function in T2 cells, we used bone marrow (BM) transplants to generate mice in which the lungs contained chimeric mixtures of wild-type and *Abcg1*$^{-/-}$ cells. Further, we generated mice lacking ABCG1 in either T2 cells (*Abcg1*$^{\text{T2-KO}}$) or macrophages (*Abcg1*$^{\text{MAC-KO}}$). Analyses of these various mice identify differential, but critical, roles for ABCG1 in both T2 cells and macrophages that affect pulmonary lipid and surfactant homeostasis and immunoglobulin levels.

MATERIALS AND METHODS

Mice

Abcg1$^{\text{flox/flox}}$ mice created on a C57BL6/J background [from Dr. Catherine Hedrick, La Jolla Institute for Allergy and Immunology (38)] were crossed with *Sftpc-Cre* mice [from Dr. Brigid Hogan, Duke University (39)] to obtain *Sftpc-Cre*$^{+}$ *Abcg1*$^{\text{flox/flox}}$ and control *Sftpc-Cre*$^{-}$ *Abcg1*$^{\text{flox/flox}}$ mice. *Abcg1*$^{\text{flox/flox}}$ mice were crossed with *LysM-Cre* mice (catalog 004781; Jackson Laboratory) to obtain *LysM-Cre*$^{+}$ *Abcg1*$^{\text{flox/flox}}$ and control *LysM-Cre*$^{-}$ *Abcg1*$^{\text{flox/flox}}$ mice. All mice used were 12-week-old males. Mice were fed a standard rodent chow diet (Purina 5001) until weaning. At weaning, mice were fed a high cholesterol diet containing 0.2% cholesterol and 21% calories from fat (D12079B; Research Diets) for 4 weeks. Mice were bred and maintained at the University of California Los Angeles in temperature-controlled pathogen-free conditions, under a 12 h light/dark cycle. All protocols involving mice were reviewed and approved by the University of California Los Angeles Animal Research Committee.

BM chimera generation

Abcg1$^{-/-}$/*LacZ* knock-in mice on a C57Bl/6 background were maintained on a standard rodent diet (Purina 5001), as described (17, 28). For BM transplantation studies, recipient wild-type and *Abcg1*$^{-/-}$ mice (10 weeks old) were γ-irradiated with 900 rad before transplantation with cells (3×10^6) from 8- to 10-week-old donor male wild-type or *Abcg1*$^{-/-}$ animals via tail vein injection. After a 4 week recovery period, mice were fed a 21% fat and 0.2% cholesterol diet (Research Diets #D12079B) for 16 weeks.

Histopathologic analysis and immunohistochemistry

Hematoxylin-eosin staining of paraffin-embedded lung sections was performed as described (17). Morphometric analysis of T2 cells was performed with Image Pro software (Media Cybernetics, Inc.). Oil red O and filipin staining of frozen lung sections was performed as described (40). Frozen lung sections were stained with antibodies for macrophages (anti-mac3 1:1,000; BD Biosciences) and T2 cells (anti-prosurfactant protein C 1:1,000; BD Biosciences). Filipin (25 μg/ml) was added during overnight

incubation of slides with antibodies. Immunostaining of adjacent sections in the absence of primary antibody was used as a negative control.

Electron microscopy

Fixed tissues were incubated with 2.5% glutaraldehyde and 2% paraformaldehyde in 100 mM cacodylate buffer (pH 7.4) overnight. Samples were then treated with 1% osmium tetroxide in 100 mM cacodylate buffer for 1 h, washed in distilled water four times (10 min/wash), and then treated with 1–2% aqueous uranyl acetate overnight at 4°C in the dark. Samples were then washed and sequentially dehydrated with increasing concentrations of acetone (20, 30, 50, 70, 90, and 100%) for 30 min each, followed by three additional treatments with 100% acetone for 20 min each. Samples were then infiltrated with increasing concentrations of Spurr's resin (25% for 1 h, 50% for 1 h, 75% for 1 h, 100% for 1 h, 100% overnight at room temperature), and then incubated overnight at 70°C in a resin mold. Sections of 50–90 nm were cut on a Leica ultramicrotome with a diamond knife. Imaging then took place using an FEI Talos F200X operating at 200 kV.

T2 pneumocyte isolation

Mouse lung cells were isolated as previously described (41), with some modifications. Lungs were perfused with PBS via the right ventricle. Lungs were inflated with enzyme solution [collagenase type I (450 U/ml; Roche Applied Science), dispase II (5 U/ml; StemCell Technologies), DNase I (0.33 U/ml; Sigma-Aldrich), and elastase (4 U/ml; Roche Applied Science)] for 3 min. Lungs were removed and minced into small pieces and incubated at 37°C for 25 min with shaking. Enzymatically digested samples were passed through needles and filtered through a 70 μM cell strainer (Fisher Scientific). After treatment with red blood cell lysis buffer, cells were filtered through a 40 μM cell strainer (Fisher Scientific) and resuspended in DMEM (Invitrogen) containing 10% FBS (Omega Scientific), 100 U/ml penicillin (Invitrogen), and 100 μg/ml streptomycin sulfate (Invitrogen). Hematopoietic cells were depleted from the lung cell suspension using the autoMACS separator with anti-mouse CD45 antibody-coated micro-beads according to the manufacturer's instructions (Miltenyi Biotech). Sorted $CD45^-$ lung cells were stained with phosphatidylethanolamine (PE)-anti-mouse epithelial cell adhesion molecule (EpCAM; eBioscience; catalog #12-5791-83; Clone G8.8) and Alex Fluor 488-anti-mouse Podoplanin/T1α (eBioscience; catalog #53-5381-82; Clone 8.1.1). T2 pneumocytes were classified as $EpCAM^{hi}/T1a^-$, as previously described (41).

RNA isolation and analysis

RNA was isolated and analyzed by real-time quantitative (q) PCR, as described (40). Each qPCR assay was performed in triplicate using cDNA samples isolated from individual mice (n = 4–6 mice/group). Primer sets are available upon request. Values were normalized to 36B4.

Immunoblotting

T2 cells and alveolar macrophages were isolated from mouse lung and broncho-alveolar lavage (BAL) fluid, respectively, as described, and lysed with RIPA buffer (Boston Bioproducts) containing protease inhibitors [25 μg/ml N-acetyl-L-leucyl-L-leucyl-L-norleucinal, 10 μg/ml leupeptin, 1 μg/ml pepstatin, and 1 mM phenylmethylsulfonyl fluoride (Sigma-Aldrich)]. Protein quantification was performed using BCA protein assay reagent (Thermo Fisher Scientific). Forty milligrams of protein per sample were loaded into SDS-PAGE and sequentially immunoblotted with anti-ABCG1 antibody (1:1,000; catalog NB400-132; Novus Biologicals).

Surfactant isolation

Pulmonary surfactant was isolated by BAL, as previously described (28). Briefly, tracheas were exposed and cannulated before the lungs were flushed three times with 1 ml aliquots of BAL buffer [10 mM Tris, 100 mM NaCl, and 0.2 mM EGTA (pH 7.2)]. The aliquots were combined and centrifuged (200 *g*, 5 min) to separate surfactant and alveolar cells.

Lipid measurements

Plasma cholesterol and triglycerides were measured using an enzymatic kit (Wako Chemicals) according to the manufacturer's instructions. Tissue lipids were extracted into $CHCl_3$ by a modified Folch method, and quantitated using enzymatic kits for cholesterol, triglycerides, or phospholipid using the accompanying protocols (Wako Chemicals).

Cholesterol and phospholipid analysis

Cells, BAL fluid, or lung tissue was snap-frozen in liquid nitrogen. Lung tissue was homogenized on ice in PBS. Cell suspensions, BAL fluid, or lung homogenates were subsequently subjected to modified Bligh-Dyer extraction (42) in the presence of lipid class internal standards, including eicosanoic acid, cholesteryl heptadecanoate, and 1,2-dieicosanoyl-*sn*-glycero-3-phosphocholine (43). Fatty acids were converted to their pentofluorobenzyl esters and subsequently quantified using GC-MS with negative-ion chemical ionization using methane as the reactant gas (44). For phospholipids, lipid extracts were diluted in methanol/chloroform (4/1, v/v) and molecular species were quantified by ESI-MS/MS on a triple quadrupole instrument (Thermo Fisher Quantum Ultra) using shotgun lipidomics methodologies (45). PC molecular species were quantified as sodiated adducts in the positive-ion mode using neutral loss scanning for 59.1 amu (collision energy = −28 eV). Neutral loss scanning for 368.5 amu (collision energy = −25 eV) was performed for quantification of sodiated CE molecular species in positive ion mode. Individual molecular species were quantified by comparing the ion intensities of the individual molecular species to that of the lipid class internal standard, with additional corrections for type I and type II [^{13}C] isotope effects (45).

A549 lipid analysis

Total lipids were extracted from 50 mg whole lung tissue and quantified, as previously described (17). A549 cells were seeded in 12-well plates (1×10^6 cells/well) and were infected overnight with either control GFP adenovirus, or adenovirus expressing ABCG1. Cells were then incubated in medium (0.2% BSA or 10% FBS) supplemented with 1 μCi/ml [^{14}C]acetate (50–60 mCi/mmol) for the indicated time. Cells were washed two times in PBS and incubated in medium (0.2% BSA or 10% FBS) ± secretagogue mixture [100 μM ATP, 0.1 μM phorbol-12-myristate-13-acetate, and 20 μM terbutaline (46)]. After the indicated time, the cells were washed three times in PBS. Lipids were extracted from the medium and cells using the Bligh and Dyer method (42). Extracted lipids were dissolved in chloroform (100 μl), and aliquots (30 μl) were analyzed by thin-layer chromatography, as described (47, 48).

Measurement of antibody titers

Total antibody titers were determined by chemiluminescent enzyme immunoassays, as previously described (49). In brief, capture antigens were coated on plates at 5 μg/ml in PBS overnight at 4°C [IgM (1:100 goat anti-mouse IgM; Sigma-Aldrich), IgG (1:400 goat anti-mouse IgG; Pierce Protein Biology), IgG1 (1:250

goat anti-mouse IgG1; Jackson ImmunoResearch Laboratories), IgG (1:250 goat anti-mouse IgG2c; Jackson ImmunoResearch Laboratories), IgA (1:100 goat anti-mouse IgA; Sigma-Aldrich)]. Plates were blocked with 1% BSA in TBS, and serially diluted antiserum or BAL fluid from individual mice was added. Plates were incubated for 1.5 h at room temperature. Bound immunoglobulin isotype levels were assessed with various anti-mouse Ig isotype-specific alkaline phosphatase conjugates using Lumi-Phos 530 (Lumigen, Southfield, MI) solution and a Dynex luminometer (Dynex Technologies, Chantilly, VA). Several secondary antibodies were used at dilutions of 1:30,000. These included alkaline phosphatase-labeled goat anti-mouse IgM (μ-chain specific), goat anti-mouse IgG (γ-chain specific), and goat anti-mouse IgA (α-chain specific) (all from Sigma-Aldrich). Specific controls were used for each specific antibody, and formal antibody dilution curves were determined in an initial study to identify the linear range of each antibody titer measurement. It was determined from these dilution curves that plasma samples could be optimally measured at 1:250 to 1:1,000 dilutions and BAL fluid samples could be optimally measured at 1:5 to 1:250 dilutions to yield concentrations within the linear detection range for each assay.

Human alveolar macrophage analysis

Human BAL fluid was collected at the University of California Los Angeles, Division of Pulmonary and Critical Care Medicine from patients with pulmonary alveolar proteinosis (PAP) undergoing whole lung lavage. Enrolled patients included both men and women, aged 42–59 years, who had previously been diagnosed with PAP and presented for a medically necessary whole lung lavage (see supplemental Table S1 for a general characterization of the human subjects group studied). Pulmonary surfactant and alveolar macrophages were isolated by centrifugation (200 *g*, 5 min). Genomic DNA was isolated from alveolar macrophages using the DNeasy extraction kit (Qiagen) according to manufacturer's instructions. *ABCG1* regulatory regions were sequenced by Sanger sequencing (GENEWIZ, LLC). Primers are available on request.

Treatment of human macrophages

Human macrophages were plated in 6-well plates in DMEM supplemented with 10% FBS, 100 U/ml penicillin, and 100 μg/ml streptomycin sulfate (medium A) on day 0. On day 1, cells were placed in medium A in the presence or absence of 1 μM GW3965 for 0, 0.5, 1, 2, 4, or 8 h. Cells were harvested in QIAZOL (Invitrogen) and total RNA extracted according to the manufacturer's instructions. Gene expression was analyzed by real-time qPCR. Each qPCR assay was performed in triplicate using cDNA samples isolated from replicate wells (n = 3 replicate wells per treatment and time point). Primer sets are available upon request. Values were normalized to 36B4.

Statistical analysis

Significance was measured, as stated, by either one-way ANOVA followed by Bonferroni correction, two-way ANOVA followed by Bonferroni correction, or by Student's *t*-test.

Study approval

Animal use was approved by the University of California Los Angeles and followed the National Institutes of Health *Guide for the Care and Use of Laboratory Animals*. All experiments were approved by the University of California Los Angeles Institute for Animal Care and Use Committee. Informed consent was obtained from human subjects for the use of BAL samples, with the approval of the Institutional Review Board for Medical Research at the University of California Los Angeles.

RESULTS

BM transplant studies identify an important role for ABCG1 expression in nonhematopoietic-derived cells

ABCG1 is highly expressed in T1 and T2 epithelial cells, interstitial and alveolar macrophages, and endothelial cells (17, 28, 40). Given the widespread expression of ABCG1 within the lung, it was not possible to determine which cell types contribute to the morphologic and lipid abnormalities observed in the lungs of *Abcg1*$^{-/-}$ mice (17, 28, 40). Previous studies indicated that accumulation of Oil red O-positive neutral lipids in the lung was greatly attenuated following BM transplantation of wild-type donor BM into recipient *Abcg1*$^{-/-}$ mice (30). This led to the proposal that the pulmonary lipidosis and inflammation were solely dependent on the presence of *Abcg1*$^{-/-}$ macrophages in the lungs of the recipient mice (30). Based on the high expression of ABCG1 in pulmonary T2 cells and the critical role these cells play in surfactant metabolism, we have reevaluated the role of ABCG1 in T2 cell function and pulmonary lipidosis.

In initial studies, we performed BM transplants using wild-type and *Abcg1*$^{-/-}$ mice as donors and/or recipients (**Fig. 1A**). This approach resulted in chimeric mice in which the lungs of the transplanted mice contain either: *i*) all *Abcg1*$^{+/+}$ cells (wild-type phenotype); *ii*) all *Abcg1*$^{-/-}$ cells (*Abcg1*$^{-/-}$ phenotype); *iii*) *Abcg1*$^{+/+}$ epithelial and endothelial cells and *Abcg1*$^{-/-}$ macrophages/lymphocytes (*Abcg1*$^{M/L\text{-}KO}$); or *iv*) *Abcg1*$^{+/+}$ macrophages/lymphocytes and *Abcg1*$^{-/-}$ epithelial and endothelial cells (*Abcg1*$^{EEC\text{-}KO}$). After BM transplantation, mice were allowed to recover for 4 weeks on a standard chow diet before being fed a high fat/high cholesterol (HF/HC) diet for 16 weeks (21% fat, 0.2% cholesterol) (Fig. 1A).

As expected, lungs of *Abcg1*$^{+/+}$ mice were morphologically normal and lacked any Oil red O-positive lipid droplets (supplemental Fig. S1A). In contrast, but consistent with earlier studies (17, 28), the lungs of mice containing *Abcg1*$^{-/-}$ macrophages exhibited reduced alveolar spaces, especially in the sub-pleural areas, as well as accumulation of Oil red O-positive cells (supplemental Fig. S1B, D). Importantly, histological analysis of the lungs of *Abcg1*$^{EEC\text{-}KO}$ chimeric mice (wild-type BM → *Abcg1*$^{-/-}$ mice) indicates that they were structurally abnormal, despite the absence of Oil red O-positive cells (supplemental Fig. S1C). **Table 1** shows that lung weights of *Abcg1*$^{-/-}$, *Abcg1*$^{M/L\text{-}KO}$, and *Abcg1*$^{EEC\text{-}KO}$ mice were increased by 82, 19, and 20%, respectively, in comparison to wild-type lungs. Further, the levels of free and esterified cholesterol as well as phospholipids were significantly increased in all three experimental groups (*Abcg1*$^{-/-}$ > *Abcg1*$^{M/L\text{-}KO}$ and *Abcg1*$^{EEC\text{-}KO}$). These data indicate that abnormal lipid homeostasis occurs not only when pulmonary macrophages and/or lymphocytes lack ABCG1, but also when ABCG1 is deleted from epithelial T1 and T2 cells and endothelial cells (*Abcg1*$^{EEC\text{-}KO}$ mice).

T2 cells lacking ABCG1 accumulate unesterified cholesterol

The finding that the lungs of *Abcg1*$^{EEC\text{-}KO}$ mice (containing wild-type macrophages/lymphocytes and *Abcg1*$^{-/-}$ epithelial

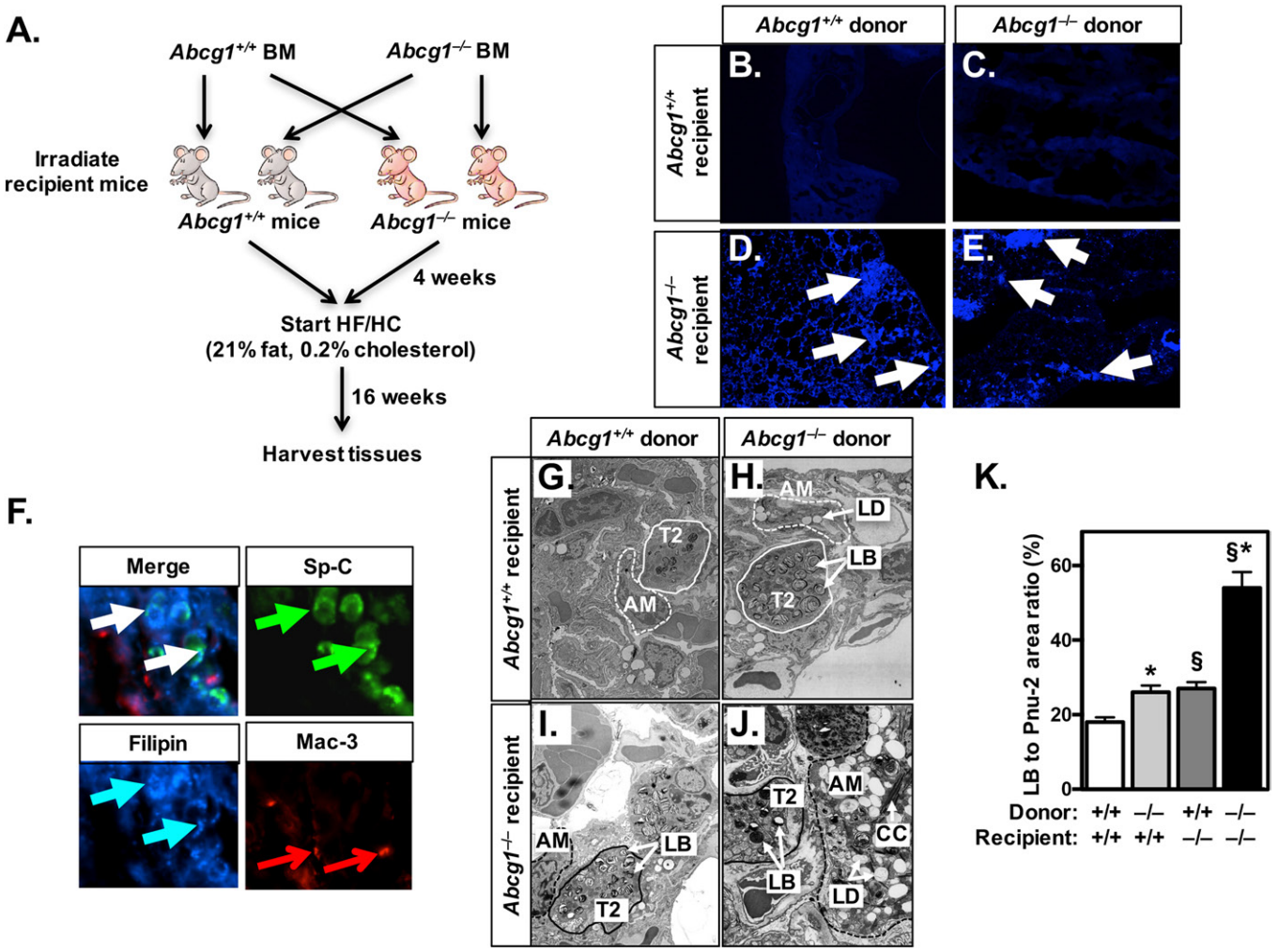

Fig. 1. ABCG1 has a critical role in nonhematopoietic cells. A: Schematic of BM transplantation studies. Wild-type and *Abcg1*$^{-/-}$ mice were irradiated and received BM from either wild-type or *Abcg1*$^{-/-}$ donor animals. After a 4 week recovery period, all mice were fed a HF/HC (21% fat, 0.2% cholesterol) diet for 16 weeks. B–E: Frozen lung sections (10 μM) of BM-transplanted mice [as in (A)] were stained with filipin for the presence of free cholesterol. White arrows mark filipin-positive areas. Images are at 20× magnification. F: Frozen lung sections (10 μM) from *Abcg1*$^{EEC\text{-}KO}$ mice (*Abcg1*$^{-/-}$ mice receiving *Abcg1*$^{+/+}$ BM) were stained with antibodies for T2 cells (pro-SP-C; green arrows) and macrophages (Mac-3; red arrows), followed by staining with filipin (blue arrows) for free cholesterol. White arrows indicate areas of colocalization. Images are at 100× magnification. G–J: Representative electron micrographs (original magnification: 9,900×) from BM-transplanted mice [as in (A)]. K: The relative area of lamellar bodies within each T2 cell was determined in electron micrographs (n = 32) from each group of transplanted mice (G–J). Significance was measured by two-way ANOVA followed by Bonferroni correction. Data are expressed as mean ± SEM. $^{*}P < 0.01$ wild-type versus *Abcg1*$^{-/-}$ donor; $^{\S}P < 0.01$ wild-type versus *Abcg1*$^{-/-}$ recipient. AM, alveolar macrophage; CC, cholesterol crystal; LB, lamellar body; LD, lipid droplet.

and endothelial cells) contained a high ratio of unesterified: total cholesterol (Table 1, column 3) was unexpected because excess unesterified cholesterol is generally toxic to cells and, hence, usually esterified and stored in lipid droplets (50). To determine whether unesterified cholesterol deposition (Table 1) localized to a specific cell type, we performed filipin staining using frozen lung sections from BM-transplanted mice. Filipin staining was only observed in the lungs of *Abcg1*$^{EEC\text{-}KO}$ and *Abcg1*$^{-/-}$ mice (Fig. 1D, E) suggesting that unesterified cholesterol was accumulating in endothelial and/or epithelial cells. Consequently, we costained frozen sections from the lungs of *Abcg1*$^{EEC\text{-}KO}$ mice with filipin and antibodies against SP-C or Mac-3 that identify T2 cells and macrophages, respectively (Fig. 1F). The data show colocalization of filipin staining with SP-C (Fig. 1F; white arrows). Thus, we conclude that the filipin-positive cells are T2 cells and that these cells have unusually high levels of unesterified cholesterol in the lungs of *Abcg1*$^{EEC\text{-}KO}$ mice fed a HF/HC diet.

Pulmonary *Abcg1*$^{-/-}$ T2 cells are abnormal in the presence of wild-type macrophages

We previously demonstrated that *Abcg1*$^{-/-}$ mice showed altered pulmonary surfactant metabolism, including increased lipid and protein levels in pulmonary surfactant recovered from BAL and abnormal T2 cells that contained increased numbers of enlarged electron-dense lamellar bodies (28). To our knowledge, it is not known whether these dramatic changes in T2 cells were a result of the loss of ABCG1 from T2 cells, macrophages, or both cell types.

TABLE 1. Altered lipid content of the lungs of bone-marrow transplanted mice

	Wild-type Recipient		*Abcg1*$^{-/-}$ Recipient	
	Wild-type Donor	*Abcg1*$^{-/-}$ Donor	Wild-type Donor	*Abcg1*$^{-/-}$ Donor
Lung weight (mg)	41.2 ± 1.2	48.4 ± 1.4[a]	50.7 ± 2.0[b]	75.7 ± 2.4[a,b]
Lung lipids (μg/mg)				
Total cholesterol	0.66 ± 0.1	2.56 ± 0.2[a]	3.32 ± 0.6[b]	8.34 ± 1.3[a,b]
Unesterified cholesterol	0.46 ± 0.1	1.04 ± 0.1[a]	2.84 ± 0.4[b]	3.42 ± 0.4[b]
Esterified cholesterol	0.20 ± 0.1	1.52 ± 0.2[a]	0.48 ± 0.2	4.92 ± 1.4[a,b]
Phospholipids	1.86 ± 0.3	4.34 ± 0.4[a]	6.50 ± 1.1[b]	11.09 ± 2.7[a,b]

Tissue lipid levels were determined as described in the Materials and Methods. Data are expressed as mean ± SEM (n = 4–6 mice/group). Significance was determined by two-way ANOVA followed by Bonferroni correction.

[a] $P < 0.01$ wild-type versus *Abcg1*$^{-/-}$ donor.

[b] $P < 0.01$ wild-type versus *Abcg1*$^{-/-}$ recipient.

Morphometric analysis of electron micrographs revealed that the T2 cells of *Abcg1*$^{-/-}$ mice had a 3-fold increase in lamellar bodies (Fig. 1J, K). These data are consistent with a prior study showing a 5-fold increase in lamellar bodies per T2 cell in the lungs of old whole-body *Abcg1*$^{-/-}$ mice (28). We now report that the T2 cells in both the *Abcg1*$^{EEC\text{-}KO}$ (Fig. 1I, K) and *Abcg1*$^{M/L\text{-}KO}$ (Fig. 1H, K) chimeric mouse models contain a 47% increase in lamellar bodies. Taken together, these data suggest that ABCG1 plays critical cell-specific roles in both T2 cells and macrophages. It also suggests that T2 cell function can be modulated by signals from alveolar macrophages that lack ABCG1.

Specific loss of ABCG1 from T2 cells has broad effects on lung morphology and gene expression

The above studies do not allow us to attribute the observed abnormalities to individual cell types. To directly define the specific role and importance of ABCG1 in the lung, we first crossed *Abcg1*$^{flox/flox}$ mice with mice expressing *Sftptc-Cre* to generate mice in which ABCG1 was specifically deleted from T2 cells (*Abcg1*$^{T2\text{-}KO}$). The fresh weight of lungs from *Abcg1*$^{T2\text{-}KO}$ mice was increased by 50%, as compared with *Abcg1*$^{flox/flox}$ mice (**Fig. 2A**) indicating that loss of ABCG1 from T2 cells has a dramatic effect on lung development and/or metabolism. This effect occurs even though T2 cells represent only ~15% of the cells in the lung and cover <5% of the alveolar surface (51). Further analysis of the lungs of *Abcg1*$^{T2\text{-}KO}$ mice indicated that they had altered histopathology consistent with sub-pleural proliferation (supplemental Fig. S2A), and did not stain with Oil red O, indicating that the tissue did not accumulate neutral lipids (supplemental Fig. S2B). Detailed morphometric analysis of multiple electron micrographs (n = 28) from the lungs of *Abcg1*$^{flox/flox}$ and *Abcg1*$^{T2\text{-}KO}$ mice demonstrates that the lungs of *Abcg1*$^{T2\text{-}KO}$ mice contain a 3-fold increase in the number of T2 cells (Fig. 2B, C) and a 2.5-fold increase in the number of lamellar bodies per T2 cell (Fig. 2B, D). In contrast, alveolar macrophages in the lungs of the *Abcg1*$^{T2\text{-}KO}$ mice appeared normal (Fig. 2B).

We performed positive selection followed by FACS to isolate cell populations highly enriched in either T2 or CD45^{+} cells (Fig. 2E). T2 cells isolated from *Abcg1*$^{T2\text{-}KO}$ mice showed an approximate 75% decrease in both the *Abcg1* mRNA and protein (Fig. 2F, G). This effect was cell-type specific because *Abcg1* mRNA in CD45^{+} cells was similar in cells isolated from control *Abcg1*$^{flox/flox}$ and *Abcg1*$^{T2\text{-}KO}$ mice (Fig. 2H). Consistent with the observed increases in T2 cells and lamellar bodies in the lungs of *Abcg1*$^{T2\text{-}KO}$ mice (Fig. 2B–D), we noted a 2.8-fold increase in *Abca3* mRNA expression in freshly isolated T2 cells lacking *Abcg1* (Fig. 2I). *Abca1* mRNA levels were also increased (Fig. 2I), likely as compensation for the loss of *Abcg1*, as previously observed in *Abcg1*$^{-/-}$ mice (28). Isolated T2 cells lacking ABCG1 also displayed decreased mRNA levels corresponding to *Srebp-2* and *Srebp-2* target genes (*Fdps* and *Ldlr*) (Fig. 2J), suggesting increased levels of sterols in these cells. T2 cells lacking ABCG1 also showed increased expression of a number of inflammatory markers that included *Il1β*, *Il6*, and *Tnfα* (Fig. 2K). As expected, fold changes in mRNA levels in extracts from the whole lungs of *Abcg1*$^{T2\text{-}KO}$ were much smaller than the changes observed in isolated T2 cells lacking *Abcg1* (compare supplemental Fig. S3A–C to Fig. 2I–K).

Loss of ABCG1 from T2 cells increases surfactant and immunoglobulin levels

We have previously reported that the lungs of *Abcg1*$^{-/-}$ mice accumulate excess B-1a B cells and natural antibodies (52). We now demonstrate that BAL fluid from *Abcg1*$^{T2\text{-}KO}$ mice contains increased titers of IgG (**Fig. 3A**), IgG2c (Fig. 3B), and IgA (Fig. 3C). These changes were specific because the levels of IgG1 and IgM were similar in the lungs of *Abcg1*$^{flox/flox}$ and *Abcg1*$^{T2\text{-}KO}$ mice (Fig. 3D, E). Plasma immunogloblulin levels were unchanged in *Abcg1*$^{T2\text{-}KO}$ mice (supplemental Fig. S3D–F).

To determine whether the abnormalities observed in lamellar body and surfactant in *Abcg1*$^{T2\text{-}KO}$ mice were associated with disruptions in intracellular lipid homeostasis, we performed lipidomic analyses on BAL fluid and T2 cells. The data show that there were significant increases in total cholesterol, cholesteryl ester, and PC levels in the surfactant of *Abcg1*$^{T2\text{-}KO}$ mice (Fig. 3F). These increases corresponded to the 18:2 and 18:1 cholesterol ester species and the 32:1 and 34:1 PC species (Fig. 3G, H). In contrast, the lipid content of T2 cells or alveolar macrophages isolated from control and *Abcg1*$^{T2\text{-}KO}$ mice were not significantly different (supplemental Fig. S3G, H). However, the decreased levels of *Srebp-2* target genes suggest that despite minimal differences in total cellular cholesterol, there may still be changes in intracellular cholesterol distribution. Together

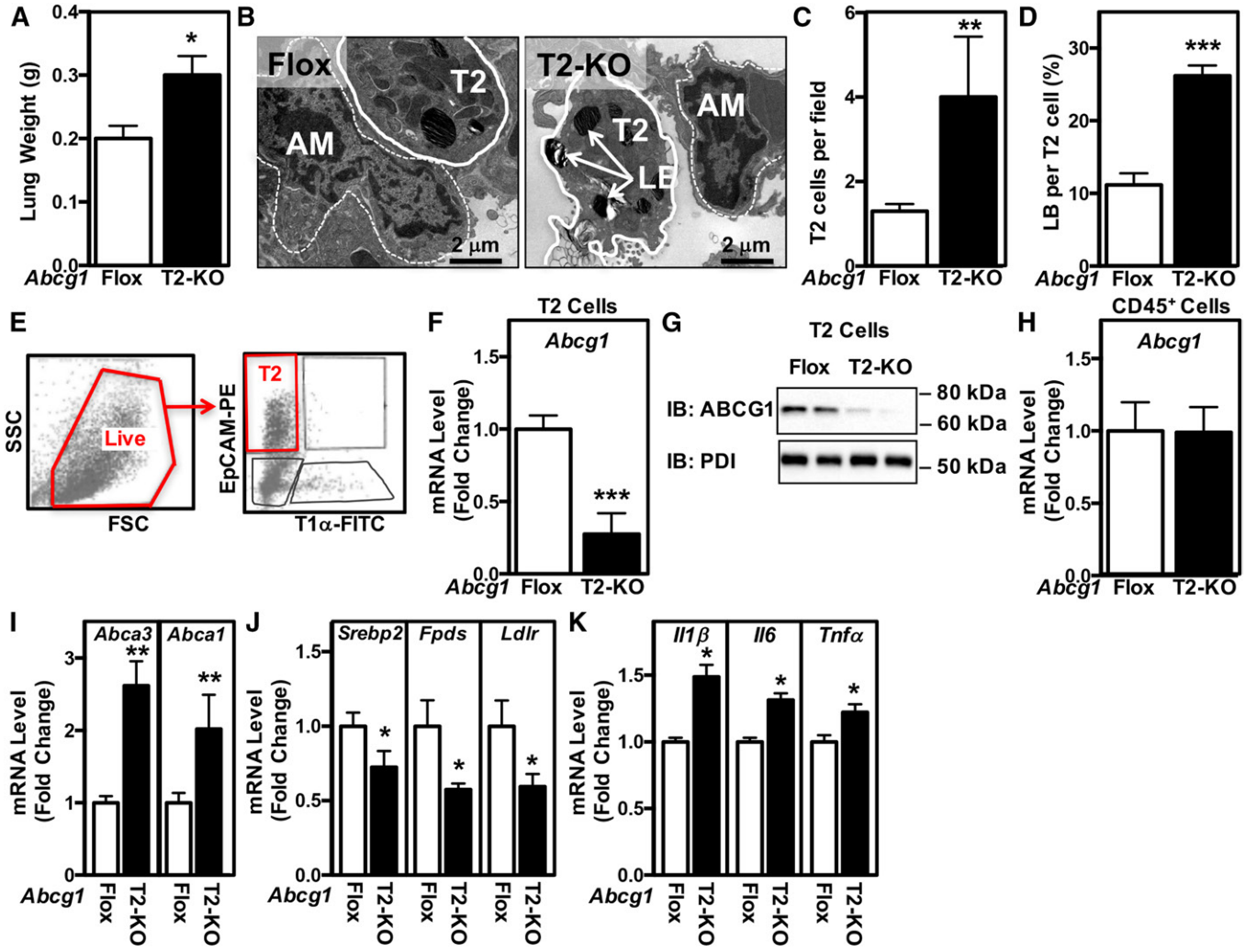

Fig. 2. Mice with selective deletion of *Abcg1* in T2 cells have abnormal surfactant and lamellar body homeostasis. A: The fresh weight of the lungs was increased in *Abcg1*$^{T2\text{-}KO}$ mice. B: Representative electron micrographs from *Abcg1*$^{flox/flox}$ and *Abcg1*$^{T2\text{-}KO}$ mice (original magnification: 17,400×). Increased T2 cell number (C) and relative area of lamellar bodies within each T2 cell (D). E: Flow cytometry gating strategy to identify T2 cells (defined as EpCAM^{hi}T1α^{-} cells). Single-cell suspensions of negatively selected CD45^{-} cells were stained with fluorophore-conjugated antibodies and analyzed by flow cytometry. Among single cells, the live cells were selected for further analysis to identify T2 cells (EpCAM^{hi}T1α^{-}). F: *Abcg1* expression is significantly reduced in EpCAM^{hi}T1α^{-} T2 cells. G: ABCG1 protein is absent from EpCAM^{hi}T1α^{-} T2 cells. H: *Abcg1* expression is unchanged in CD45^{+} cells isolated from *Abcg1*$^{T2\text{-}KO}$ mice. I: Increased *Abca3* and *Abca1* expression in EpCAM^{hi}T1α^{-} T2 cells. J: Decreased *Srebp-2*, *Fdps*, and *Ldlr* expression in EpCAM^{hi}T1α^{-} T2 cells. K: Increased *Il1β*, *Il6*, and *Tnfα* expression in EpCAM^{hi}T1α^{-} T2 cells. Significance was measured by Student's *t*-test. Data are expressed as mean ± SEM. *$P < 0.05$, **$P < 0.01$, ***$P < 0.001$.

these data suggest that ABCG1 in T2 cells has a critical role that affects pulmonary and surfactant lipid homeostasis, as well as modulating the immune response.

Expression of ABCG1 in A549 cells alters lipid synthesis and secretion

The studies presented here demonstrate that ABCG1 plays a critical role in T2 cell biology and homeostasis. The human-derived A549 cell line exhibits a number of T2-like properties, including the presence of lamellar body-like organelles and the ABC transporter, ABCA3 (53). In addition, treatment of A549 cells with secretogogues increases secretion of lamellar bodies/phospholipids into the media (54). To determine whether ABCG1 affects synthesis and secretion of specific lipids, we infected A549 cells with control adenovirus or ABCG1 adenovirus (Ad-ABCG1). After 24 h, cells were incubated with ^{14}C-acetate for 6 h in medium containing 0.2% BSA (data not shown) or 10% FBS prior to quantification of radioactive cell-associated lipids (**Fig. 4A**, B). The data of Fig. 4A, B show that overexpression of ABCG1 results in increased incorporation of ^{14}C-acetate into cholesterol (Fig. 4A, B; 46–52%), consistent with our earlier observation that overexpression of ABCG1 increases cholesterol synthesis genes (24, 55). Further, overexpression of ABCG1 increased incorporation of ^{14}C-acetate into FFA and DG (Fig. 4A; 71% and 74%, respectively), as well as PC (15%), PE (13%), PA/PS phospholipids (10%), and SM (20%) (Fig. 4B). The incorporation of ^{14}C-acetate into triacylglycerol, phosphatidylglycerol (PG), and PI remained largely unchanged (Fig. 4B). Similar results were seen with 0.2% BSA-containing medium (data not shown).

In a second series of experiments, we determined the role of ABCG1 in surfactant secretion. A549 cells were infected with control adenovirus or Ad-ABCG1, as in Fig. 4A, B.

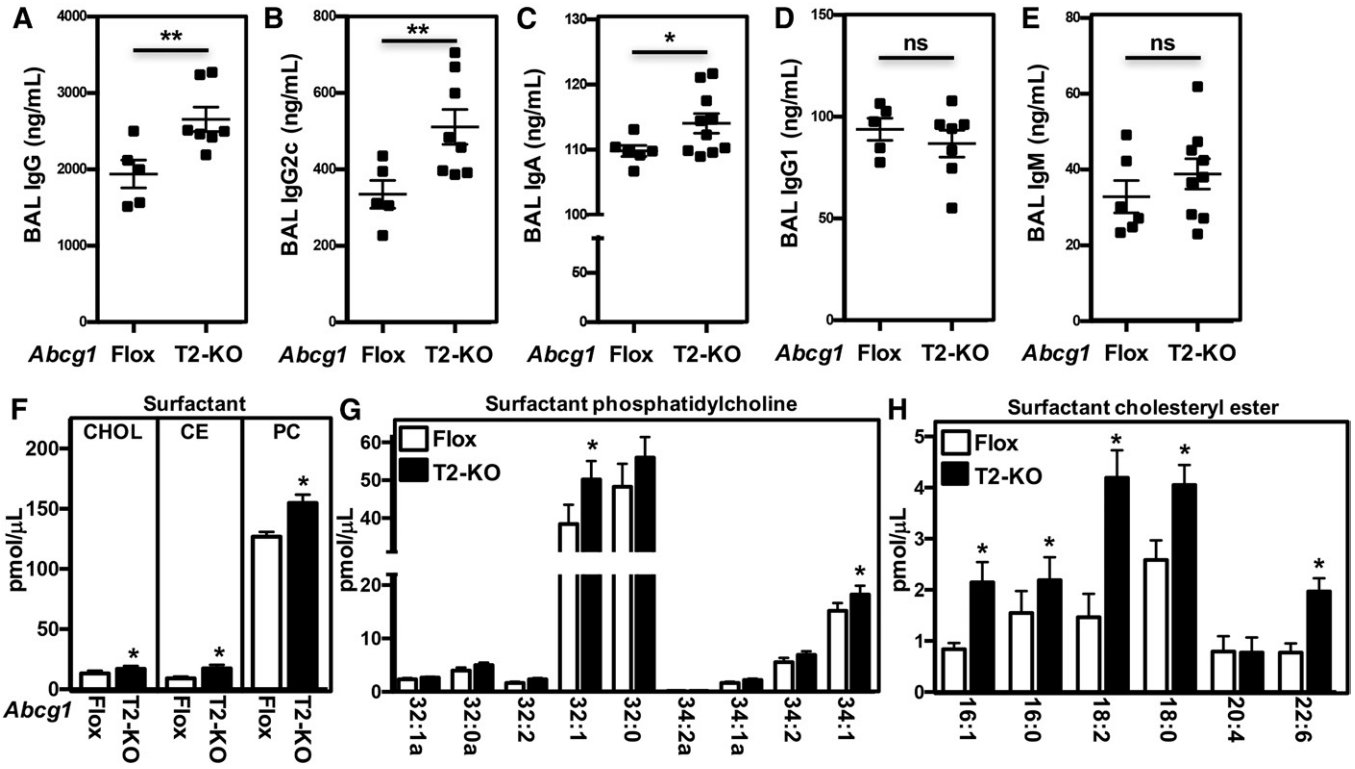

Fig. 3. Disrupted lipid homeostasis and immunity in *Abcg1*$^{T2\text{-}KO}$ mice. A–E: BAL fluid from *Abcg1*$^{flox/flox}$ and *Abcg1*$^{T2\text{-}KO}$ mice was diluted 1:5 to 1:250 and tested for binding to IgG (A), IgA (B), IgG2c (C), IgG1 (D), and IgM (E). ALP-conjugated antibodies were used for detection. Data are presented as mean antibody titer (ng/ml) ± SEM (n = 5–10 mice/genotype). F–H: Cholesterol, cholesteryl ester, and PC and their derivatives were quantified by ESI-MS/MS in BAL fluid from *Abcg1*$^{flox/flox}$ and *Abcg1*$^{T2\text{-}KO}$ mice. Data are presented as mean lipid level (pmol/µl) ± SEM (n = 3–6 mice/genotype). Significance was measured by Student's *t*-test. $^{*}P < 0.05$, $^{**}P < 0.01$.

After 24 h, cells were pulsed with ^{14}C-acetate for 4 h to label newly synthesized lipids. Cells were washed and chased for 2 h in medium containing either 0.2% BSA (supplemental Fig. S4A) or 10% FBS (Fig. 4C) in the presence or absence of a surfactant secretagogue cocktail (28). Consistent with the secretion of lamellar bodies, the cocktail increased secretion of PC (38%), PE (85%), SM (66%), and cholesterol (85%) into the medium (Fig. 4C; supplemental Fig. S4A, lanes 5, 6 vs. 1, 2 and lanes 7, 8 vs. 3, 4). ABCG1 overexpression increased secretion of both cholesterol (248%) and PC (33%), independent of whether the cells were incubated in lipid-free medium (supplemental Fig. S4A, 0.2% BSA; lanes 3, 4) or medium containing exogenous lipid acceptors (Fig. 4C, 10% FBS; lanes 3, 4).

Lastly, we determined the role of silencing ABCG1 on lipid secretion. A549 cells were transfected with a scrambled siRNA sequence or siRNA sequences targeted against *ABCG1* (Fig. 4D). Consistent with our observations in *Abcg1*$^{T2\text{-}KO}$ mice (Fig. 2I), silencing *ABCG1* in A549 cells resulted in compensatory increases in *ABCA1* and *ABCA3* mRNA (supplemental Fig. S4B). Silencing *ABCG1* in A549 cells resulted in increased total cellular cholesterol and phospholipids (Fig. 4E), and decreased cholesterol and phospholipid secretion into the medium (Fig. 4F).

Abcg1$^{-/-}$ macrophages modulate wild-type T2 cell surfactant homeostasis

Data from our BM transplant studies suggested that T2 cell function can be modulated by signals from alveolar macrophages and/or lymphocytes that lack ABCG1. To test this hypothesis, we generated conditional KO mice in which ABCG1 was selectively deleted in macrophages using *LysM-Cre*. ABCG1 deletion in alveolar macrophages was confirmed by mRNA expression and Western blotting (**Fig. 5A**, B). As expected, and consistent with previous studies (28, 30, 40), *Abcg1*$^{MAC\text{-}KO}$ lungs displayed altered histopathology, increased proliferation in the sub-pleural space, and accumulation of Oil red O-positive macrophages (supplemental Fig. S5A, B). Morphological analysis of the lungs from *Abgc1*$^{MAC\text{-}KO}$ mice demonstrated the accumulation of giant alveolar macrophages filled with lipid droplets and cholesterol crystals (Fig. 5C). Upon closer inspection of individual micrographs, we noted that the T2 cells in the lungs of *Abcg1*$^{MAC\text{-}KO}$ mice were also enlarged with multiple irregularly shaped and electron dense lamellar bodies (Fig. 5D). Quantification of T2 cells and lamellar bodies demonstrated that *Abcg1*$^{MAC\text{-}KO}$ lungs have 4-fold more T2 cells (Fig. 5E), and each T2 cell contained 2.2-fold more lamellar bodies (Fig. 5F). These data suggest that the absence of ABCG1 specifically from macrophages also significantly impacts T2 lamellar body and surfactant homeostasis.

ABCG1 human variants in PAP

Overall, our data demonstrate that ABCG1 plays a critical role in normal T2 cell and surfactant homeostasis in mice. Importantly, we wanted to determine whether ABCG1 is important in pulmonary surfactant metabolism in humans. Chronic respiratory diseases are the third leading cause of

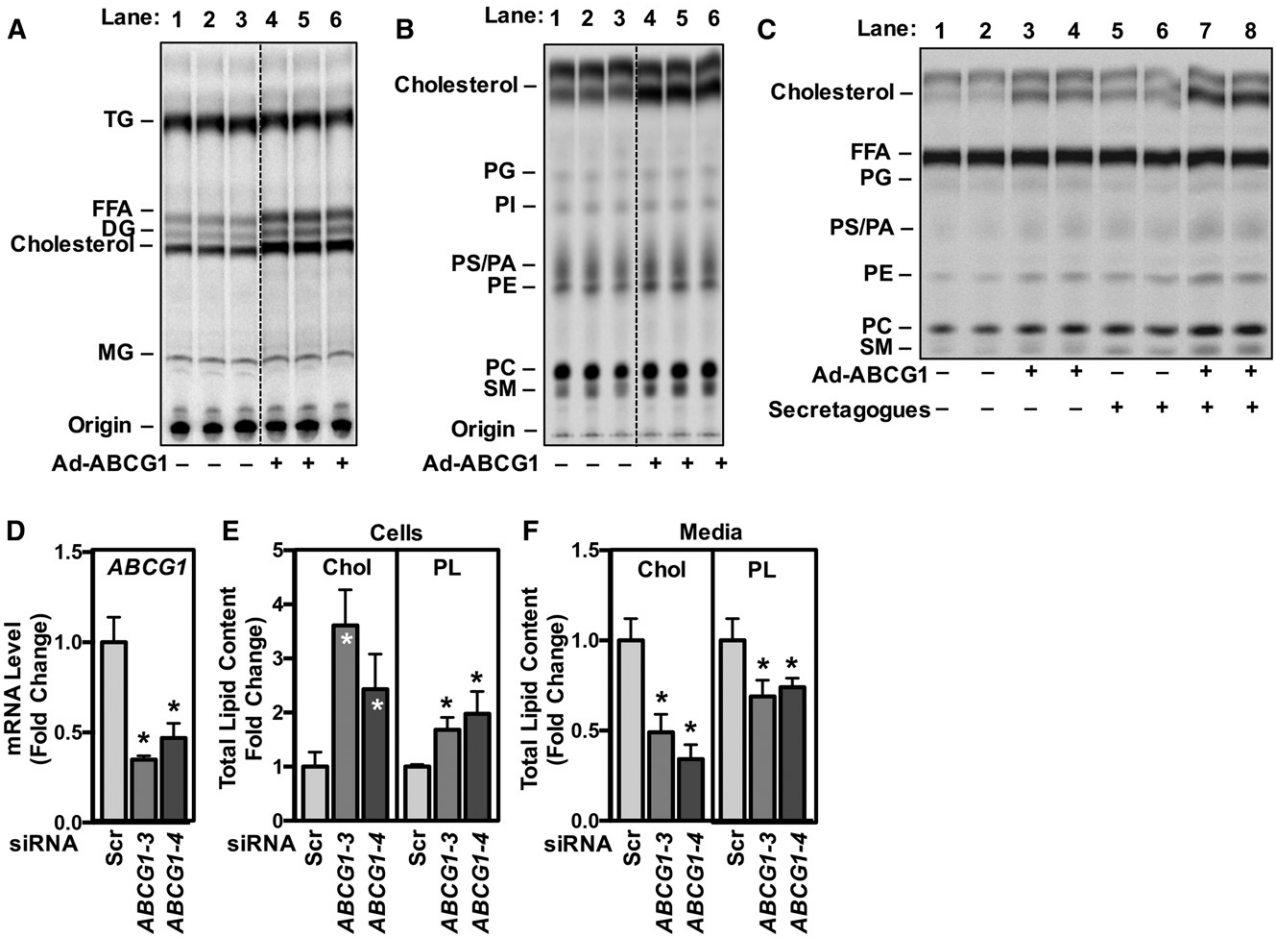

Fig. 4. ABCG1 is required for the synthesis and secretion of cholesterol and phospholipids from A549 T2 cells. A, B: A549 T2 cells were infected overnight with either control adenovirus or Ad-ABCG1. Cells were incubated with ^{14}C-acetate in medium containing 10% FBS for 6 h before total cellular lipids were extracted and separated by thin-layer chromatography to determine levels of neutral lipids (A) and phospholipids (B). C: A549 T2 cells were infected as in (A, B). Cells were pulse labeled with ^{14}C-acetate for 4 h, followed by a 2 h chase in medium containing 10% FBS in the presence or absence of a secretagogue cocktail (100 μM ATP, 0.1 μM phorbol-12-myristate-13-acetate, 20 μM terbutaline). Total secreted lipids were extracted from the medium and separated by thin-layer chromatography to determine the levels of phospholipids. D–F: A549 T2 cells were transfected with a control scrambled siRNA sequence or siRNA sequences directed against *ABCG1*. D: Reduced *ABCG1* expression in A549 cells treated with *ABCG1* siRNA. Total cellular (E) and secreted (F) cholesterol and phospholipids were quantified by enzymatic assay according to manufacturer's instructions. Data are presented as mean ± SEM (n = 6 replicates/condition). Significance was measured by one-way ANOVA followed by Bonferroni correction. $^{*}P < 0.01$.

death (56), and PAP is a rare disease caused by the accumulation of SPs and lipids in the pulmonary alveoli, resulting in respiratory distress (57, 58). Patients with autoimmune idiopathic PAP have reduced alveolar macrophage expression of *ABCG1* (59) and exhibit a remarkable resemblance to the phenotype observed in the lungs of *Abcg1*$^{-/-}$ mice. We hypothesized that polymorphisms in the human *ABCG1* locus may result in decreased ABCG1 function and, subsequently, altered pulmonary function.

We obtained human BAL samples from PAP patients undergoing whole lung lavage at the University of California Los Angeles. Information on the human subjects is detailed in supplemental Table S1. Genomic DNA isolated from patient alveolar macrophages was sequenced and compared with published reference sequences (NCBI). We found multiple sequence polymorphisms in one PAP patient, which correspond to a region containing a putative liver X receptor (LXR) response element (**Fig. 6A**) (60). LXRα is a well-known regulator of macrophage function (61, 62). To determine whether this sequence polymorphism affected the response to LXR activation, we generated luciferase reporter genes in which the 2,000 bp upstream of the *ABCG1* transcriptional start site containing the published reference or mutated putative LXRE sequence were inserted upstream of the luciferase coding sequence (Fig. 6B, C). Plasmids containing these reporter genes and expression plasmids for LXRα and RXRα were transfected into HEK293 cells, and the cells treated for 24 h with either LXR and RXR agonists or vehicle. Figure 6B shows that LXR activation resulted in a significant increase in luciferase activity with the reference plasmid. However, no significant increase in luciferase activity was observed with the plasmid containing the mutated LXRE sequence (Fig. 6C). We next treated control or PAP patient macrophages with LXRα agonist for the indicated time period (**Fig. 7**). ABC transporter gene expression was determined by real-time qPCR. The data of Fig. 7A demonstrate that induction of *ABCG1* mRNA levels by a specific LXRα

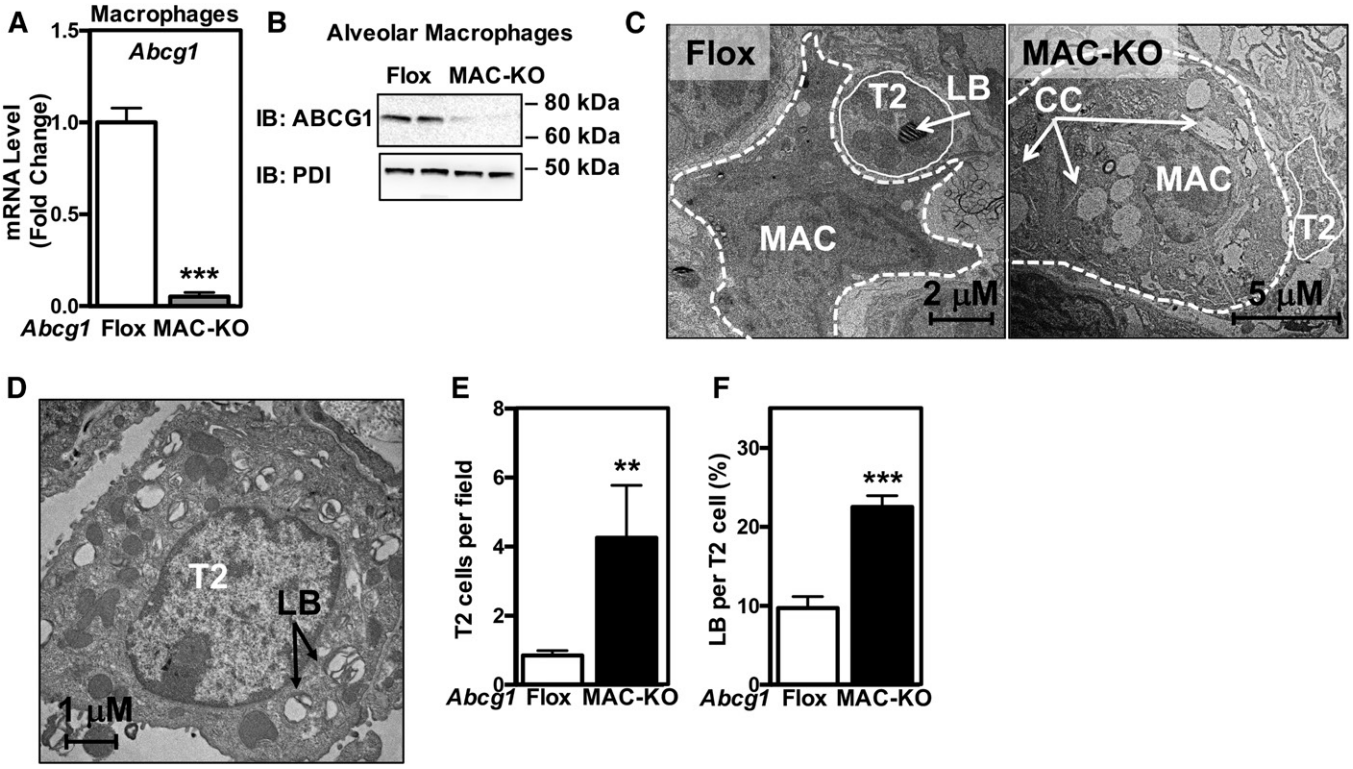

Fig. 5. *Abcg1*$^{-/-}$ macrophages signal to wild-type T2 cells. A, B: ABCG1 is absent in alveolar macrophages isolated from *Abcg1*$^{\text{MAC-KO}}$ mice. A: *Abcg1* expression in alveolar macrophages isolated from *Abcg1*$^{\text{flox/flox}}$ and *Abcg1*$^{\text{MAC-KO}}$ mice. B: ABCG1 protein in alveolar macrophages isolated from *Abcg1*$^{\text{flox/flox}}$ and *Abcg1*$^{\text{MAC-KO}}$ mice. C: Representative electron micrographs from *Abcg1*$^{\text{flox/flox}}$ and *Abcg1*$^{\text{MAC-KO}}$ mice (original magnification: 17,400×). D: Electron micrograph of a T2 cell from *Abcg1*$^{\text{MAC-KO}}$ mice (original magnification: 22,600×). Increased T2 cell number (E) and relative area of lamellar bodies within each T2 cell (F) in *Abcg1*$^{\text{MAC-KO}}$ mice. Data are expressed as mean ± SEM (n = 4–6 mice/genotype). AM, alveolar macrophage; CC, cholesterol crystal; LB, lamellar body; T2, T2 cell. Significance was measured by Student's *t*-test. $^{**}P < 0.01$, $^{***}P < 0.001$.

agonist were significantly impaired in PAP patient macrophages (Fig. 7A), while minimal differences were noted in the induction of other LXR target genes, including *ABCA1*, *IDOL*, and *LPCAT3* (Fig. 7B–D). Together these data suggest that the sequence polymorphism identified within the *ABCG1* locus could be, in part, responsible for the reduced ABCG1 function observed in PAP patient macrophages (Fig. 7) (59).

DISCUSSION

Improper pulmonary lipid homeostasis results in different respiratory syndromes, such as PAP, respiratory distress of the newborn, idiopathic pulmonary fibrosis, or chronic obstructive pulmonary disease (34, 35, 63–67). Studies in both patients and mice have identified GM-CSF, SP-B, SP-C, SP-D, ABCA3, ABCA1, and lysosomal acid lipase (LAL) as genes involved in some of these syndromes (32, 34, 35, 63, 65–67). We previously reported a severe lipidosis in the lungs of aged *Abcg1*$^{-/-}$ mice fed a normal chow diet (28). *Abcg1*$^{-/-}$ lungs accumulated foamy macrophages and abnormal T2 cells, and displayed massive deposition of cholesterol (both unesterified and esterified) and phospholipids. Additionally, severe signs of inflammation that included lymphocytic infiltration and increased expression of cytokines were observed in the lungs of *Abcg1*$^{-/-}$ mice. Interestingly, this phenotype could be accelerated in younger animals by feeding a HF/HC diet (17).

An important question that remained to be established in those studies was the relative importance of alveolar macrophages and T2 cells for the development of the lung phenotype in *Abcg1*$^{-/-}$ mice. The presence of a *LacZ* knock-in cassette, under transcriptional control of the endogenous *Abcg1* promoter, allowed us to unequivocally identify both alveolar macrophages and T2 cells that normally express ABCG1 (17, 28). Wojcik et al. (30) previously reported that, following BM transplants, Oil red O deposition and cytokine induction in the murine lungs correlated with the presence of *Abcg1*$^{-/-}$ BM-derived cells, independent of the genotype of the recipient mice. However, we note that, in contrast to the study reported herein, the mice studied by Wojcik et al. (30) were not challenged with a HF/HC diet, were euthanized after only 9 weeks post-transplantation, and the lipid content of T2 cells was not reported.

Here we show that ABCG1 is critical for surfactant and T2 cell homeostasis. *Abcg1*$^{\text{T2-KO}}$ mice allowed us to specifically study the function of ABCG1 in T2 cells, while use of *Abcg1*$^{\text{MAC-KO}}$ and BM chimeras allowed us to study the contribution of ABCG1 in other lung cell types, such as macrophages. Our results are consistent with previous reports (30) that loss of ABCG1 expression in BM-derived cells leads to deposition of Oil red O-positive lipids (i.e., cholesteryl esters)

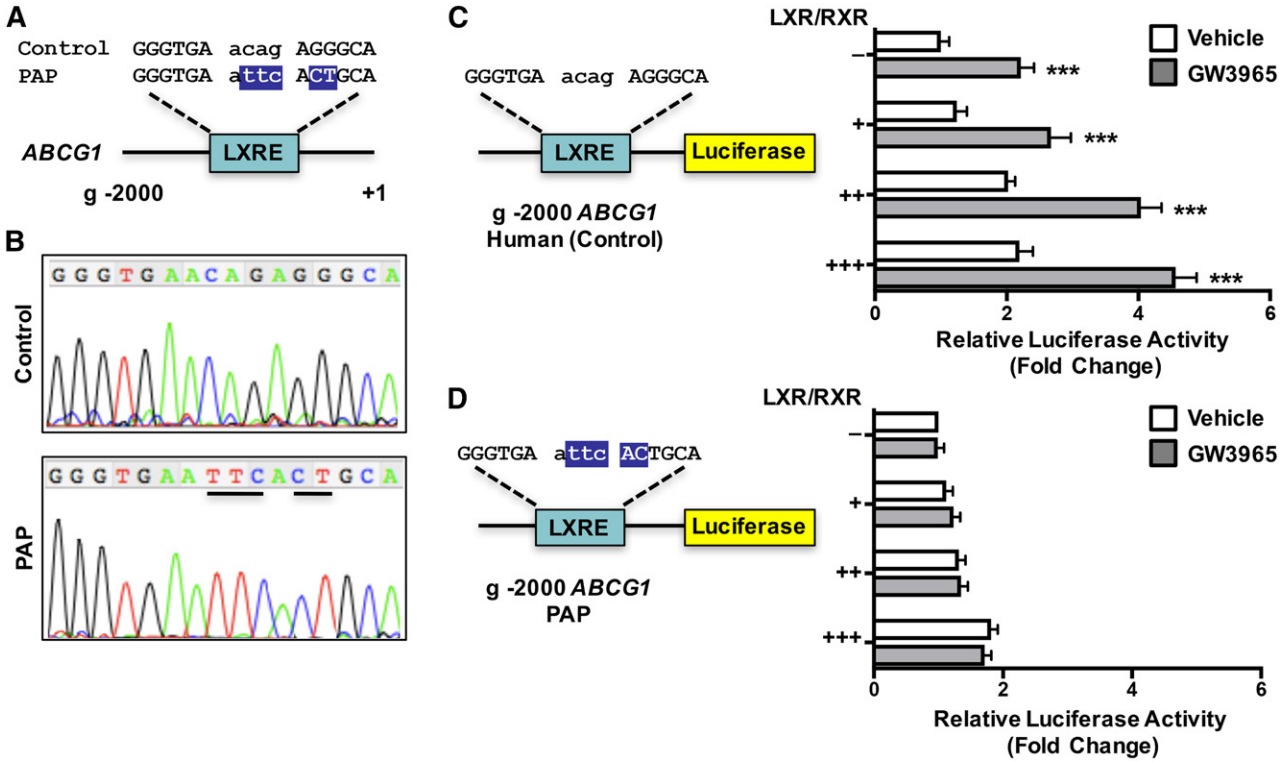

Fig. 6. Sequence polymorphisms in human *ABCG1* in patients with PAP. A: Genomic location of *ABCG1* sequence polymorphisms. B: Sequence trace from control or PAP patient showing sequence polymorphisms. C, D: The 2,000 bp upstream of the *ABCG1* transcriptional start site was cloned upstream of the luciferase gene from control and PAP patient genomic DNA. The reporter plasmid was transfected into CHO-K1 cells together with a β-galactosidase expression plasmid and increasing amounts of LXRα and RXRα expression plasmids in the presence or absence of LXRα agonist, GW3965 (1 μM). Promoter activity was normalized to β-galactosidase activity. Data are presented as mean ± SEM. Significance was measured by Student's *t*-test. ***$P < 0.001$.

in pulmonary macrophages (supplemental Fig. S1, Table 1). In addition to these observations, we demonstrate that, under conditions of dietary challenge with a HF/HC diet, loss of ABCG1 function in alveolar T2 cells results in increased lamellar body content, and increased pulmonary phospholipids and unesterified cholesterol (Fig. 1, Table 1). These results highlight the importance of ABCG1 function not just in alveolar macrophages, but also in T2 cells. The data also suggest that loss of ABCG1 in either cell type results in phenotypic changes related to pulmonary lipid homeostasis. Therefore, perhaps not surprisingly, total loss of the transporter in the lungs (*Abcg1*$^{-/-}$ BM → *Abcg1*$^{-/-}$ recipient mice) leads to a more severe phenotype (Fig. 1, supplemental Fig. S1, Table 1).

T2 cell-specific ABCG1-deficient mice accumulated abnormal electron-dense lamellar bodies, and had increased surfactant levels of cholesteryl ester, PC, and immunoglobulins (Figs. 2, 3). These data demonstrate that ABCG1 expression in T2 cells not only regulates T2 surfactant lipid homeostasis, but also immune response and immunoglobulins, consistent with previous reports that ABCG1 plays important roles in both lipid homeostasis and immunity (30, 38, 52, 68–74). Loss of ABCG1 in T2 cells compromises their ability to secrete and/or recycle surfactant lipids, resulting in hypertrophied cells that accumulate enlarged lamellar bodies [(28) and this study]. We have previously shown that continual uptake of cholesterol-rich surfactant by *Abcg1*$^{-/-}$ macrophages, coupled with impaired macrophage cholesterol efflux, results in the generation of macrophage foam cells (28). These data strongly suggest that the phenotype observed in *Abcg1*$^{-/-}$ mice is the result of not only cell-specific events, but also complex interactions between the different pulmonary cell types, particularly alveolar macrophages and T2 cells.

LacZ staining of frozen sections from mice lacking ABCG1 revealed that ABCG1 is also expressed in endothelial cells and epithelial cells lining the bronchioles (17, 27, 28, 40). It is likely that alterations in these cells as a result of loss of ABCG1 expression may also contribute to the phenotype observed in the lungs of *Abcg1*$^{-/-}$ mice. Endothelial cells are known to produce and secrete numerous cytokines in response to a variety of stimuli [reviewed in (75)]. Some of these molecules have been described to modulate monocyte/macrophage migration and/or T2 cell proliferation in the lungs during inflammation or following tissue damage (75). The role of such crosstalk between endothelial cells and macrophages and T2 cells in the lungs remains to be elucidated.

To our knowledge, no functional mutations have been described in human *ABCG1*. However, Thomassen et al. (76) reported that a subgroup of patients with PAP showed a marked decrease in ABCG1 mRNA expression in alveolar macrophages recovered from BALs, compared with samples from healthy volunteers. This same group has also demonstrated that lentiviral overexpression of ABCG1 improves the lipid-loaded macrophage phenotype of *Gmcsf*$^{-/-}$ mice

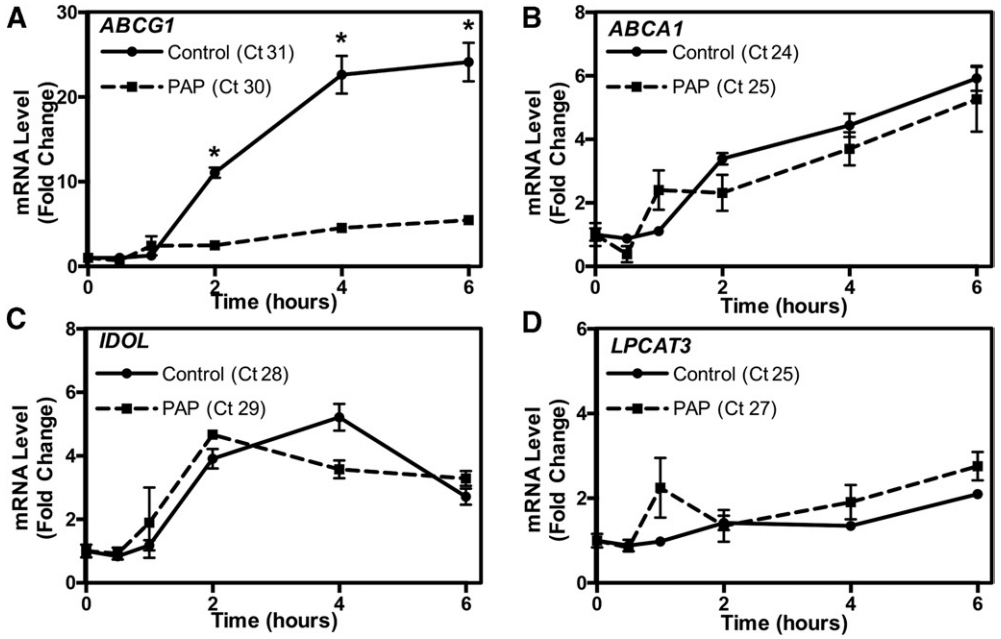

Fig. 7. Reduced activation of ABCG1 by LXR in a patient with PAP. A–D: Macrophages isolated from a PAP patient and non-PAP control were plated and treated with a specific LXR agonist (1 μM GW3965) for the indicated time period. *ABCG1* (A), *ABCA1* (B), *IDOL* (C), and *LPCAT3* (D) activation by LXR. Gene expression was normalized to 36B4 and presented as fold changes. Data are presented as mean ± SEM. Significance was measured by two-way ANOVA followed by Bonferroni correction. $^*P < 0.001$.

(77). Importantly, we identified sequence polymorphisms in ABCG1 in one PAP patient that correspond to a putative LXR response element. We show that the normal induction of *ABCG1* mRNA in response to LXR activation was greatly attenuated in alveolar macrophages isolated from one PAP patient (Fig. 7). In contrast, induction of other LXR target genes, including *ABCA1*, *IDOL*, and *LPCAT3*, in control and patient-derived cells were not significantly different. These data suggest that polymorphisms that affect the expression and/or function of ABCG1 may result in an increased risk of pulmonary lipidosis and inflammation.

In summary, our results identify a critical role for ABCG1 in controlling T2 cell surfactant metabolism and pulmonary immunoglobulin levels. We also identify sequence polymorphisms in *ABCG1* in a human patient with PAP that impact the regulation of *ABCG1* expression by LXR. Our data suggest that a decline in pulmonary ABCG1 levels may affect the pathogenesis of PAP. Finally, the current studies support the proposal that altering intracellular cholesterol metabolism in T2 cells affects both surfactant secretion/recycling and pulmonary immunity.

The authors thank Drs. Peter Edwards and Joseph Witztum, and members of the Tarling laboratory for critical reading of the manuscript. The authors thank Tony Mottino from the Department of Medicine at University of California Los Angeles for electron microscopy technical assistance. The authors would like to acknowledge Columbia University's Nanoscience Initiative (CNI) for the use of its shared facilities and the Fu Foundation School of Engineering and Applied Science and the Faculty of Arts and Sciences for their support of the CNI facilities.

REFERENCES

1. Schürch, S., M. Lee, and P. Gehr. 1992. Pulmonary surfactant: surface properties and function of alveolar and airway surfactant. *Pure Appl. Chem.* **64:** 1745–1750.
2. Chander, A., and A. B. Fisher. 1990. Regulation of lung surfactant secretion. *Am. J. Physiol.* **258:** L241–L253.
3. Haagsman, H. P., A. Hogenkamp, M. van Eijk, and E. J. A. Veldhuizen. 2008. Surfactant collectins and innate immunity. *Neonatology.* **93:** 288–294.
4. McIntosh, J. C., A. H. Swyers, J. H. Fisher, and J. R. Wright. 1996. Surfactant proteins A and D increase in response to intratracheal lipopolysaccharide. *Am. J. Respir. Cell Mol. Biol.* **15:** 509–519.
5. Wright, J. R. 2004. Host defense functions of pulmonary surfactant. *Biol. Neonate.* **85:** 326–332.
6. Wright, J. R. 2005. Immunoregulatory functions of surfactant proteins. *Nat. Rev. Immunol.* **5:** 58–68.
7. Weaver, T. E., C-L. Na, and M. Stahlman. 2002. Biogenesis of lamellar bodies, lysosome-related organelles involved in storage and secretion of pulmonary surfactant. *Semin. Cell Dev. Biol.* **13:** 263–270.
8. Mason, R. J., M. C. Lewis, K. E. Edeen, K. McCormick-Shannon, L. D. Nielsen, and J. M. Shannon. 2002. Maintenance of surfactant protein A and D secretion by rat alveolar type II cells in vitro. *Am. J. Physiol. Lung Cell. Mol. Physiol.* **282:** L249–L258.
9. Hass, M. A., and W. J. Longmore. 1979. Surfactant cholesterol metabolism of the isolated perfused rat lung. *Biochim. Biophys. Acta.* **573:** 166–174.
10. Goerke, J. 1998. Pulmonary surfactant: functions and molecular composition. *Biochim. Biophys. Acta.* **1408:** 79–89.
11. Gurel, O., M. Ikegami, Z. Chroneos, and A. Jobe. 2001. Macrophage and type II cell catabolism of SP-A and saturated phosphatidylcholine in mouse lungs. *Am. J. Physiol. Lung Cell. Mol. Physiol.* **280:** L1266–L1272.
12. Baldán, A., P. Tarr, R. Lee, and P. A. Edwards. 2006. ATP-binding cassette transporter G1 and lipid homeostasis. *Curr. Opin. Lipidol.* **17:** 227–232.
13. Baldán, A., D. D. Bojanic, and P. A. Edwards. 2009. The ABCs of sterol transport. *J. Lipid Res.* **50:** S80–S85.
14. Tarr, P. T., E. J. Tarling, D. D. Bojanic, P. A. Edwards, and A. Baldan. 2009. Emerging new paradigms for ABCG transporters. *Biochim. Biophys. Acta.* **1791:** 584–593.

15. Tarling, E. J., and P. A. Edwards. 2012. Dancing with the sterols: critical roles for ABCG1, ABCA1, miRNAs, and nuclear and cell surface receptors in controlling cellular sterol homeostasis. *Biochim. Biophys. Acta.* **1821:** 386–395.
16. Gelissen, I. C., M. Harris, K-A. Rye, C. Quinn, A. J. Brown, M. Kockx, S. Cartland, M. Packianathan, L. Kritharides, and W. Jessup. 2006. ABCA1 and ABCG1 synergize to mediate cholesterol export to apoA-I. *Arterioscler. Thromb. Vasc. Biol.* **26:** 534–540.
17. Kennedy, M. A., G. C. Barrera, K. Nakamura, A. Baldan, P. Tarr, M. C. Fishbein, J. Frank, O. L. Francone, and P. A. Edwards. 2005. ABCG1 has a critical role in mediating cholesterol efflux to HDL and preventing cellular lipid accumulation. *Cell Metab.* **1:** 121–131.
18. Klucken, J., C. Buchler, E. Orso, W. E. Kaminski, M. Porsch-Ozcurumez, G. Liebisch, M. Kapinsky, W. Diederich, W. Drobnik, M. Dean, et al. 2000. ABCG1 (ABC8), the human homolog of the Drosophila white gene, is a regulator of macrophage cholesterol and phospholipid transport. *Proc. Natl. Acad. Sci. USA.* **97:** 817–822.
19. Kobayashi, A., Y. Takanezawa, T. Hirata, Y. Shimizu, K. Misasa, N. Kioka, H. Arai, K. Ueda, and M. Matsuo. 2006. Efflux of sphingomyelin, cholesterol, and phosphatidylcholine by ABCG1. *J. Lipid Res.* **47:** 1791–1802.
20. Nakamura, K., M. A. Kennedy, A. Baldan, D. D. Bojanic, K. Lyons, and P. A. Edwards. 2004. Expression and regulation of multiple murine ATP-binding cassette transporter G1 mRNAs/isoforms that stimulate cellular cholesterol efflux to high density lipoprotein. *J. Biol. Chem.* **279:** 45980–45989.
21. Vaughan, A. M., and J. F. Oram. 2005. ABCG1 redistributes cell cholesterol to domains removable by high density lipoprotein but not by lipid-depleted apolipoproteins. *J. Biol. Chem.* **280:** 30150–30157.
22. Vaughan, A. M., and J. F. Oram. 2006. ABCA1 and ABCG1 or ABCG4 act sequentially to remove cellular cholesterol and generate cholesterol-rich HDL. *J. Lipid Res.* **47:** 2433–2443.
23. Wang, N., D. Lan, W. Chen, F. Matsuura, and A. R. Tall. 2004. ATP-binding cassette transporters G1 and G4 mediate cellular cholesterol efflux to high-density lipoproteins. *Proc. Natl. Acad. Sci. USA.* **101:** 9774–9779.
24. Tarling, E. J., and P. A. Edwards. 2011. ATP binding cassette transporter G1 (ABCG1) is an intracellular sterol transporter. *Proc. Natl. Acad. Sci. USA.* **108:** 19719–19724.
25. Tarling, E. J., and P. A. Edwards. 2016. Intracellular localization of endogenous mouse ABCG1 is mimicked by both ABCG1-L550 and ABCG1-P550-brief report. *Arterioscler. Thromb. Vasc. Biol.* **36:** 1323–1327.
26. Sturek, J. M., J. D. Castle, A. P. Trace, L. C. Page, A. M. Castle, C. Evans-Molina, J. S. Parks, R. G. Mirmira, and C. C. Hedrick. 2010. An intracellular role for ABCG1-mediated cholesterol transport in the regulated secretory pathway of mouse pancreatic beta cells. *J. Clin. Invest.* **120:** 2575–2589.
27. Baldán, A., A. V. Gomes, P. Ping, and P. A. Edwards. 2008. Loss of ABCG1 results in chronic pulmonary inflammation. *J. Immunol.* **180:** 3560–3568.
28. Baldán, A., P. Tarr, C. S. Vales, J. Frank, T. K. Shimotake, S. Hawgood, and P. A. Edwards. 2006. Deletion of the transmembrane transporter ABCG1 results in progressive pulmonary lipidosis. *J. Biol. Chem.* **281:** 29401–29410.
29. Out, R., M. Hoekstra, R. B. Hildebrand, J. K. Kruit, I. Meurs, Z. Li, F. Kuipers, T. J. C. Van Berkel, and M. Van Eck. 2006. Macrophage ABCG1 deletion disrupts lipid homeostasis in alveolar macrophages and moderately influences atherosclerotic lesion development in LDL receptor-deficient mice. *Arterioscler. Thromb. Vasc. Biol.* **26:** 2295–2300.
30. Wojcik, A. J., M. D. Skaflen, S. Srinivasan, and C. C. Hedrick. 2008. A critical role for ABCG1 in macrophage inflammation and lung homeostasis. *J. Immunol.* **180:** 4273–4282.
31. Out, R., M. Hoekstra, K. Habets, I. Meurs, V. de Waard, R. B. Hildebrand, Y. Wang, G. Chimini, J. Kuiper, T. J. C. Van Berkel, et al. 2008. Combined deletion of macrophage ABCA1 and ABCG1 leads to massive lipid accumulation in tissue macrophages and distinct atherosclerosis at relatively low plasma cholesterol levels. *Arterioscler. Thromb. Vasc. Biol.* **28:** 258–264.
32. Bates, S. R., J. Q. Tao, H. L. Collins, O. L. Francone, and G. H. Rothblat. 2005. Pulmonary abnormalities due to ABCA1 deficiency in mice. *Am. J. Physiol. Lung Cell. Mol. Physiol.* **289:** L980–L989.
33. Fitzgerald, M. L., R. Xavier, K. J. Haley, R. Welti, J. L. Goss, C. E. Brown, D. Z. Zhuang, S. A. Bell, N. Lu, M. Mckee, et al. 2007. ABCA3 inactivation in mice causes respiratory failure, loss of pulmonary surfactant, and depletion of lung phosphatidylglycerol. *J. Lipid Res.* **48:** 621–632.
34. Bullard, J. E., S. E. Wert, J. A. Whitsett, M. Dean, and L. M. Nogee. 2005. ABCA3 mutations associated with pediatric interstitial lung disease. *Am. J. Respir. Crit. Care Med.* **172:** 1026–1031.
35. Shulenin, S., L. M. Nogee, T. Annilo, S. E. Wert, J. A. Whitsett, and M. Dean. 2004. ABCA3 gene mutations in newborns with fatal surfactant deficiency. *N. Engl. J. Med.* **350:** 1296–1303.
36. Francis, G. A., R. H. Knopp, and J. F. Oram. 1995. Defective removal of cellular cholesterol and phospholipids by apolipoprotein A-1 in Tangier disease. *J. Clin. Invest.* **96:** 78–87.
37. Rogler, G., B. Trumbach, B. Klima, K. J. Lackner, and G. Schmitz. 1995. HDL-mediated efflux of intracellular cholesterol is impaired in fibroblasts from Tangier disease patients. *Arterioscler. Thromb. Vasc. Biol.* **15:** 683–690.
38. Cheng, H. Y., D. E. Gaddis, R. Wu, C. McSkimming, L. D. Haynes, A. M. Taylor, C. A. McNamara, M. Sorci-Thomas, and C. C. Hedrick. 2016. Loss of ABCG1 influences regulatory T cell differentiation and atherosclerosis. *J. Clin. Invest.* **126:** 3236–3246.
39. Okubo, T., P. S. Knoepfler, R. N. Eisenman, and B. L. Hogan. 2005. Nmyc plays an essential role during lung development as a dosage-sensitive regulator of progenitor cell proliferation and differentiation. *Development.* **132:** 1363–1374.
40. Tarling, E. J., D. D. Bojanic, R. K. Tangirala, X. Wang, A. Lovgren-Sandblom, A. J. Lusis, I. Bjorkhem, and P. A. Edwards. 2010. Impaired development of atherosclerosis in Abcg1-/- Apoe-/- mice: identification of specific oxysterols that both accumulate in Abcg1-/- Apoe-/- tissues and induce apoptosis. *Arterioscler. Thromb. Vasc. Biol.* **30:** 1174–1180.
41. Fujino, N., H. Kubo, T. Suzuki, C. Ota, A. E. Hegab, M. He, S. Suzuki, T. Suzuki, M. Yamada, T. Kondo, et al. 2011. Isolation of alveolar epithelial type II progenitor cells from adult human lungs. *Lab. Invest.* **91:** 363–378.
42. Bligh, E. G., and W. J. Dyer. 1959. A rapid method for total lipid extraction and purification. *Can. J. Biochem. Physiol.* **37:** 911–917.
43. Demarco, V. G., D. A. Ford, E. J. Henriksen, A. R. Aroor, M. S. Johnson, J. Habibi, L. Ma, M. Yang, C. J. Albert, J. W. Lally, et al. 2013. Obesity-related alterations in cardiac lipid profile and nondipping blood pressure pattern during transition to diastolic dysfunction in male db/db mice. *Endocrinology.* **154:** 159–171.
44. Quehenberger, O., A. Armando, D. Dumlao, D. L. Stephens, and E. A. Dennis. 2008. Lipidomics analysis of essential fatty acids in macrophages. *Prostaglandins Leukot. Essent. Fatty Acids.* **79:** 123–129.
45. Han, X., and R. W. Gross. 2005. Shotgun lipidomics: electrospray ionization mass spectrometric analysis and quantitation of cellular lipidomes directly from crude extracts of biological samples. *Mass Spectrom. Rev.* **24:** 367–412.
46. Chintagari, N. R., N. Jin, P. Wang, T. A. Narasaraju, J. Chen, and L. Liu. 2006. Effect of cholesterol depletion on exocytosis of alveolar type II cells. *Am. J. Respir. Cell Mol. Biol.* **34:** 677–687.
47. Sommerer, D., R. Süss, S. Hammerschmidt, H. Wirtz, K. Arnold, and J. Schiller. 2004. Analysis of the phospholipid composition of bronchoalveolar lavage (BAL) fluid from man and minipig by MALDI-TOF mass spectrometry in combination with TLC. *J. Pharm. Biomed. Anal.* **35:** 199–206.
48. White, T., S. Bursten, D. Federighi, R. A. Lewis, and E. Nudelman. 1998. High-resolution separation and quantification of neutral lipid and phospholipid species in mammalian cells and sera by multi-one-dimensional thin-layer chromatography. *Anal. Biochem.* **258:** 109–117.
49. Binder, C. J., S. Horkko, A. Dewan, M-K. Chang, E. P. Kieu, C. S. Goodyear, P. X. Shaw, W. Palinski, J. L. Witztum, and G. J. Silverman. 2003. Pneumococcal vaccination decreases atherosclerotic lesion formation: molecular mimicry between Streptococcus pneumoniae and oxidized LDL. *Nat. Med.* **9:** 736–743.
50. Chang, T-Y., C. C. Y. Chang, S. Lin, C. Yu, B-L. Li, and A. Miyazaki. 2001. Roles of acyl-coenzyme A: cholesterol acyltransferase-1 and -2. *Curr. Opin. Lipidol.* **12:** 289–296.
51. Castranova, V., J. Rabovsky, J. H. Tucker, and P. R. Miles. 1988. The alveolar type II epithelial cell: a multifunctional pneumocyte. *Toxicol. Appl. Pharmacol.* **93:** 472–483.
52. Baldan, A., A. Gonen, C. Choung, X. Que, T. J. Marquart, I. Hernandez, I. Bjorkhem, D. A. Ford, J. L. Witztum, and E. J. Tarling. 2014. ABCG1 is required for pulmonary B-1 B cell and natural antibody homeostasis. *J. Immunol.* **193:** 5637–5648.
53. Lieber, M., B. Smith, A. Szakal, W. Nelson-Rees, and G. Todaro. 1976. A continuous tumor-cell line from a human lung carcinoma with properties of type II alveolar epithelial cells. *Int. J. Cancer.* **17:** 62–70.

54. Shapiro, D. L., L. L. Nardone, S. A. Rooney, E. K. Motoyama, and J. L. Munoz. 1978. Phospholipid biosynthesis and secretion by a cell line (A549) which resembles type II alveolar epithelial cells. *Biochim. Biophys. Acta.* **530:** 197–207.
55. Tarr, P. T., and P. A. Edwards. 2008. ABCG1 and ABCG4 are coexpressed in neurons and astrocytes of the CNS and regulate cholesterol homeostasis through SREBP-2. *J. Lipid Res.* **49:** 169–182.
56. Centers for Disease Control and Prevention. 2011. National Diabetes Fact Sheet, 2011. Accessed March 1, 2017, at https://stacks.cdc.gov/view/cdc/13329.
57. Carey, B., and B. C. Trapnell. 2010. The molecular basis of pulmonary alveolar proteinosis. *Clin. Immunol.* **135:** 223–235.
58. Trapnell, B. C., J. A. Whitsett, and K. Nakata. 2003. Pulmonary alveolar proteinosis. *N. Engl. J. Med.* **349:** 2527–2539.
59. Thomassen, M. J., B. P. Barna, A. G. Malur, T. L. Bonfield, C. F. Farver, A. Malur, H. Dalrymple, M. S. Kavuru, and M. Febbraio. 2007. ABCG1 is deficient in alveolar macrophages of GM-CSF knockout mice and patients with pulmonary alveolar proteinosis. *J. Lipid Res.* **48:** 2762–2768.
60. Sabol, S. L., H. B. Brewer, Jr., and S. Santamarina-Fojo. 2005. The human ABCG1 gene: identification of LXR response elements that modulate expression in macrophages and liver. *J. Lipid Res.* **46:** 2151–2167.
61. Hong, C., and P. Tontonoz. 2008. Coordination of inflammation and metabolism by PPAR and LXR nuclear receptors. *Curr. Opin. Genet. Dev.* **18:** 461–467.
62. Zelcer, N., and P. Tontonoz. 2006. Liver X receptors as integrators of metabolic and inflammatory signaling. *J. Clin. Invest.* **116:** 607–614.
63. Anderson, R. A., G. M. Bryson, and J. S. Parks. 1999. Lysosomal acid lipase mutations that determine phenotype in Wolman and cholesterol ester storage disease. *Mol. Genet. Metab.* **68:** 333–345.
64. Arai, T., E. Hamano, Y. Inoue, T. Ryushi, T. Nukiwa, M. Sakatani, and K. Nakata. 2004. Serum neutralizing capacity of GM-CSF reflects disease severity in a patient with pulmonary alveolar proteinosis successfully treated with inhaled GM-CSF. *Respir. Med.* **98:** 1227–1230.
65. Lian, X., C. Yan, L. Yang, Y. Xu, and H. Du. 2004. Lysosomal acid lipase deficiency causes respiratory inflammation and destruction in the lung. *Am. J. Physiol. Lung Cell. Mol. Physiol.* **286:** L801–L807.
66. Nogee, L. M. 2004. Alterations in SP-B and SP-C expression in neonatal lung disease. *Annu. Rev. Physiol.* **66:** 601–623.
67. Bewig, B., X. Wang, D. Kirsten, K. Dalhoff, and H. Schafer. 2000. GM-CSF and GM-CSF beta c receptor in adult patients with pulmonary alveolar proteinosis. *Eur. Respir. J.* **15:** 350–357.
68. Bensinger, S. J., M. N. Bradley, S. B. Joseph, N. Zelcer, E. M. Janssen, M. A. Hausner, R. Shih, J. S. Parks, P. A. Edwards, B. D. Jamieson, et al. 2008. LXR signaling couples sterol metabolism to proliferation in the acquired immune response. *Cell.* **134:** 97–111.
69. Draper, D. W., K. M. Gowdy, J. H. Madenspacher, R. H. Wilson, G. S. Whitehead, H. Nakano, A. R. Pandiri, J. F. Foley, A. T. Remaley, D. N. Cook, et al. 2012. ATP binding cassette transporter G1 deletion induces IL-17-dependent dysregulation of pulmonary adaptive immunity. *J. Immunol.* **188:** 5327–5336.
70. Draper, D. W., J. H. Madenspacher, D. Dixon, D. H. King, A. T. Remaley, and M. B. Fessler. 2010. ATP-binding cassette transporter G1 deficiency dysregulates host defense in the lung. *Am. J. Respir. Crit. Care Med.* **182:** 404–412.
71. Armstrong, A. J., A. K. Gebre, J. S. Parks, and C. C. Hedrick. 2010. ATP-binding cassette transporter G1 negatively regulates thymocyte and peripheral lymphocyte proliferation. *J. Immunol.* **184:** 173–183.
72. Whetzel, A. M., J. M. Sturek, M. H. Nagelin, D. T. Bolick, A. K. Gebre, J. S. Parks, A. C. Bruce, M. D. Skaflen, and C. C. Hedrick. 2010. ABCG1 deficiency in mice promotes endothelial activation and monocyte-endothelial interactions. *Arterioscler. Thromb. Vasc. Biol.* **30:** 809–817.
73. Sag, D., C. Cekic, R. Wu, J. Linden, and C. C. Hedrick. 2015. The cholesterol transporter ABCG1 links cholesterol homeostasis and tumour immunity. *Nat. Commun.* **6:** 6354.
74. Sag, D., G. Wingender, H. Nowyhed, R. Wu, A. K. Gebre, J. S. Parks, M. Kronenberg, and C. C. Hedrick. 2012. ATP-binding cassette transporter G1 intrinsically regulates invariant NKT cell development. *J. Immunol.* **189:** 5129–5138.
75. Rao, R. M., L. Yang, G. Garcia-Cardena, and F. W. Luscinskas. 2007. Endothelial-dependent mechanisms of leukocyte recruitment to the vascular wall. *Circ. Res.* **101:** 234–247.
76. Thomassen, M. J., B. P. Barna, A. G. Malur, T. L. Bonfield, C. F. Farver, A. Malur, H. Dalrymple, M. S. Kavuru, and M. Febbraio. 2007. ABCG1 is deficient in alveolar macrophages of GM-CSF knockout mice and patients with pulmonary alveolar proteinosis. *J. Lipid Res.* **48:** 2762–2768.
77. Malur, A., I. Huizar, G. Wells, B. P. Barna, A. G. Malur, and M. J. Thomassen. 2011. Lentivirus-ABCG1 instillation reduces lipid accumulation and improves lung compliance in GM-CSF knock-out mice. *Biochem. Biophys. Res. Commun.* **415:** 288–293.